The Korean Journal of Rheology,
Vol. 1, No. 1, November 1989, pp.12-19.

Crystallization, Vitrification and Phase Separation During Reactive Polymer Processing

Sung Chul Kim

Department of Chemical Engineering, KAIST P.O. Box 131 Cheongryang, Seoul, Korea
(Received August 14, 1989)

Abstract—Polymer fluid flow and polymerization reaction occur simultaneously during the reactive polymer processing. The viscosity and physical properties change as the reaction proceeds and the crystallization and vitrification occur as the T_m and the T_g of the polymerizing fluid exceeds the reaction temperature within the mold.

INTRODUCTION

Reactive polymer processing includes the reaction injection molding (RIM), reactive extrusion (REX), reactive spinning, pultrusion and the BMC (bulk molding compound) and SMC (sheet molding compound) processes. The fluid flow and polymerization occur at the same time and the physical properties of the polymerizing fluid change as the reaction proceeds. The glass transition temperature (T_g) and the melting point (T_m) of the polymerizing fluid increases as the conversion increases. Thus reaction-induced crystallization occurs as the T_m of the polymerizing fluid exceeds the reaction temperature (the local temperature inside the mold cavity) in the case of the reactive processing of the semi-crystalline polymers such as Nylon 6. This process has to be kinetically expressed since the exothermic heat from the crystallization changes the temperature profile, reaction rate and the viscosity of the fluid.

The reaction-induced vitrification (solidification) occurs as the T_g of the polymerizing fluid exceeds the reaction temperature in the case of the RIM process of epoxy resin. The vitrification stops the reaction and a new kinetic equation of the curing reaction has to be derived in order to model the reactive processes. This phenomena will affect the T_g profile across the thickness direction of the molded article.

Rubber, particularly amine or carboxylated acrylonitrile butadiene rubber (ATBN or CTBN) is sometimes added to the epoxy resin to impart high impact properties. The rubber is soluble in the epoxy oligomer at the initial stage of the reactive processing but as the curing reaction proceeds and the molecular weight of the epoxy resin increases, the compatibility of epoxy and rubber decreases and at certain level of conversion, phase separation is started. the competing process of phase separation, vitrification and gellation determines the final morphology of the epoxy RIM product. The phase separation process also occurs during the polyurethane-unsaturated polyester and polyurethane-epoxy IPN RIM processes.

This paper reviews recent studies done at the polymer engineering lab. of the chemical engineering department of KAIST.

REACTION INDUCED CRYSTALLIZATION OF NYLON 6

The anionic polymerization during the reaction injection molding process of Nylon 6 is carried out somewhat below the melting point of the polymerized product, and thus the reaction induced crystallization occurs as the reaction proceeds. A nonisothermal crystallization kinetic equation was obtained (1) and the engineering analysis of the RIM process of Nylon 6 was carried out including the exothermic effect of the crystallization during the processing and the crystallinity profile in the molded product was obtained (2).

The caprolactam monomer was polymerized under anhydrous condition using sodium caprolactam as the catalyst and the activator was prepared

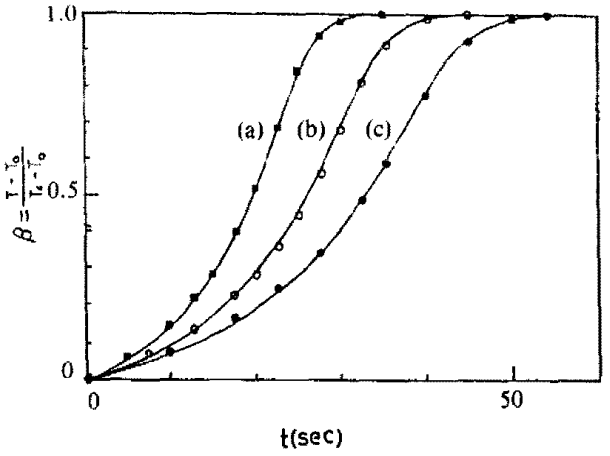

Fig. 1. Comparison of the experimental conversion data (points) and the calculated values (lines) from Eq. 3 at various initial temperatures; (a) 144.5°C, (b) 138.5°C and (c) 133.2°C.

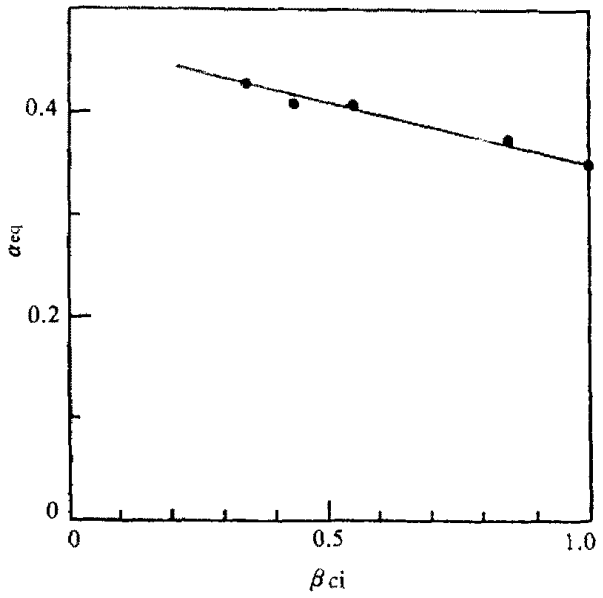

Fig. 2. Equilibrium crystallinity versus the conversion at which the crystallization started to occur.

by reacting hexamethylene diisocyanate (HDI) with caprolactam monomer at 80°C. The concentration of the catalyst and the activator were 1.5 mol% and 0.5 mol%, respectively.

The reaction kinetics for the Nylon 6 polymerization was obtained from the adiabatic experiment measuring the exothermic heat of polymerization in the case when the polymerization and crystallization occur separately (when the reaction is carried out at high thmperature, the polymerization occurs first and the crystallization is observed after the polymer is formed due to the slow rate of crystallization). The final equation was obtained by fitting the experimental results from the adiabatic experiments carried out at different initial temperatures with the autocatalytic model as follows (Eq. 1 and Fig. 1).

$$\frac{d\beta}{dt}=1.8\times10^{6}\exp\left(\frac{15800}{RT}\right)(1-\beta)(1+6.2\beta) \qquad (1)$$

A new crystallization kinetic equation was derived to describe the crystallization kinetics induced by the polymerization. In Eq. 2, the first exponential term indicated the diffusion of the polymer chain. The constant E_d was observed to increase as the molecular weight of Nylon 6 increased. The second exponential term described the supercooling effect and the melting point T_m should be expressed as a function of conversion. The fourth term was included to describe the effect off the impingement of the growing crystals.

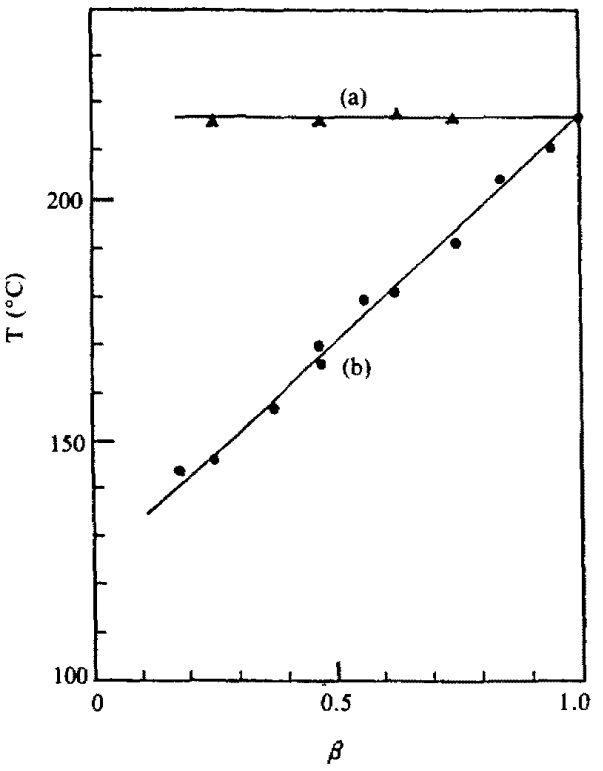

Fig. 3. Melting temperature versus conversion; (a) melting temperature of the monomer extracted polymer (b) melting temperature of the reaction mixture.

$$\frac{d\alpha}{dt}=8.33\times10^{6}\exp\left(-\frac{E_d}{RT}\right)\exp\left(-\frac{\Psi T_m}{T(T_m-T)}\right)$$
$$\alpha^{2/3}(\alpha_{eq}-\alpha) \qquad (2)$$

The α_{eq} was the equilibrium crystallinity that could be obtained at a given conversion and it was observed to vary with the initial conversion when the crystallization had started. High equilibrium crystallinity was obtained when the crystallization was started at low conversion (when the reaction temperature was low) and slightly lower equilibrium conversion was obtained when the crystallization was started after the reaction proceeded to some extent due to the viscosity effect of the medium. Fig. 2 and Eq. 3 was obtained to describe this effect.

$$\alpha_{eq} = -0.11\beta_{ri} + 0.46 \tag{3}$$

The melting point change as a function of conversion was also obtained from actual experiment by stopping the reaction at intermediate conversion and measuring the T_m of the reaction intermediate. Fig. 3 and Eq. 4 was obtained to describe this T_m change.

$$Tm = 92\beta + 125 \tag{4}$$

In order to obtain a correlation between the two constants, one for the diffusion and the other for the supercooling effect in Eq. 2, the temperature of the maximum rate of crystallization T_k was derived by differentiating the Eq. 2. And by rearranging Eq. 6, a correlation between E_d and Ψ was obtained as Eq. 7.

$$\frac{d}{dT}\left(\frac{d\alpha}{dt}\right)\Big|_{T=T_g} = 0 \tag{5}$$

$$T_g = \frac{T_m(E_d + R\Psi - \sqrt{Ru(E_d + R\Psi)})}{E_d} \tag{6}$$

$$\Psi = \frac{E_d(T_m - T_g)^2}{RT(2T_g - T_m)} \tag{7}$$

The temperature of maximum crystallization rate, T_k could be obtained by carrying out the DSC cooling experiment and measuring the peak of the exotherm during crystallization on reaction mixture with different conversion level. The crystallization peak temperature at the cooling rate of 10°C/min was obtained and it was assumed that the crystallization peak temperature at the cooling rate of 0°C/min which corresponded to the isothermal crystallization experiment should be proportional to the peak temperature measured at 10°C/min (a). From literature, it was reported that the T_k value of Nylon 6 was 140°C and the new correlation between the conversion and T_k was obtained as Eq. 8.

$$T_g = 87.8\beta + 51.2 \tag{8}$$

The actual crystallization data was obtained by carrying out the adiabatic experiments at low initial temperature to have the polymerization and kinetic data was obtained from the exothermic heat of crystallization by subtracting the exothermic heat of reaction from the overall exotherm. The parameters in Eq. 2 were determined as follows by fitting the experimental curve with the equation as shown in Fig. 4 and Eq. 9. The effect of the reaction rate constant k on the simulated exotherm from the polymerization and the crystallization by combining the Eq. 1 and 2 is shown in Fig. 5. When the polymerization rate is very fast as in line (a), the crystallization exotherm is observed after the polymerization is completed, but when the reaction is slow, the polymerization and the crystallization occur at the same time.

$$E_d = \frac{3.18}{1.64 - \beta} + 3.25\beta + 3.28 \tag{9}$$

A computer simulation for the Reaction Injection Molding (RIM) Process was conducted based on the nonisothermal reaction induced crystallization kinetic equation thus obtained in a disk type mold (2). The temperature, conversion and the crystallinity profile inside the mold cavity as a function of time were obtained as shown in Fig. 6, 7 and 8. It was observed that the conversion reached near comple-

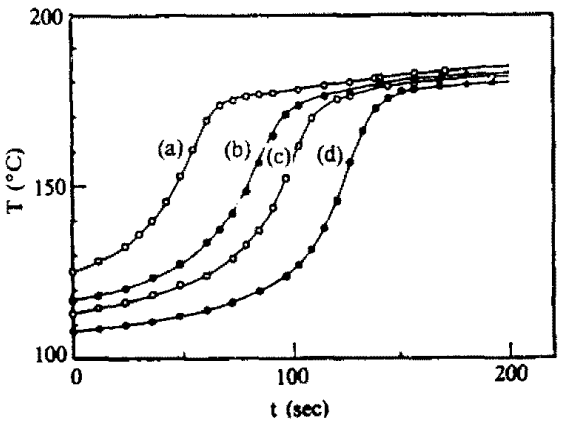

Fig. 4. Comparison of the adiabatic temperature rise between the experimental data (points) and the calculate values (lines) from Eq. 4 at various initial temperature; (a) 125.7°C, (b) 117.3°C, (c) 113.5°C, and (d) 108°C.

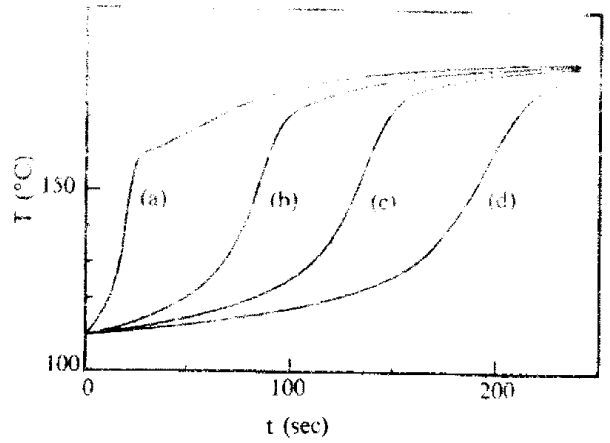

Fig. 5. Adiabatic temperature rise calculated from Eq. 4 at different value of k; (a) 1.0×10, (b) 2.5×10, (c) 1.5×10, and (d) 1.0×10 (initial temperature is set at 110°C).

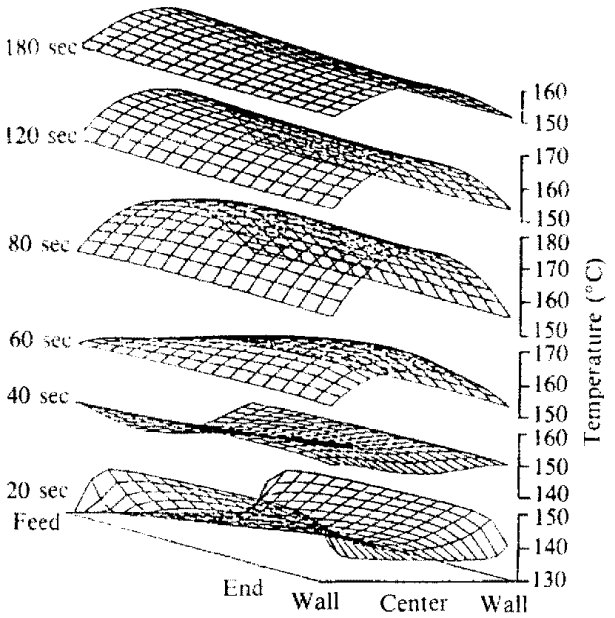

Fig. 6. Change of the temperature profile with time.

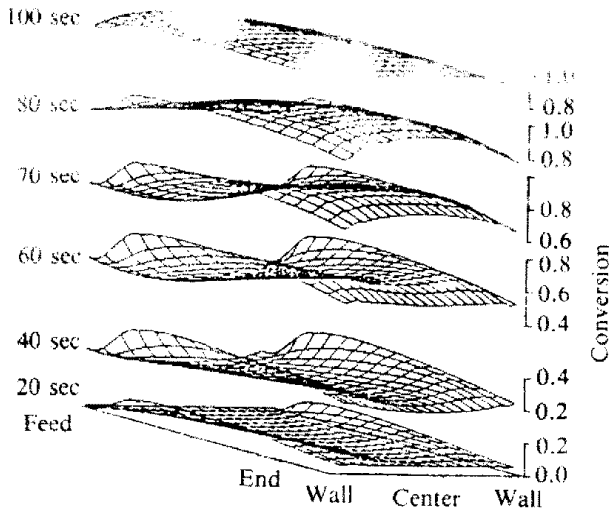

Fig. 7. Change of the conversion profile with time.

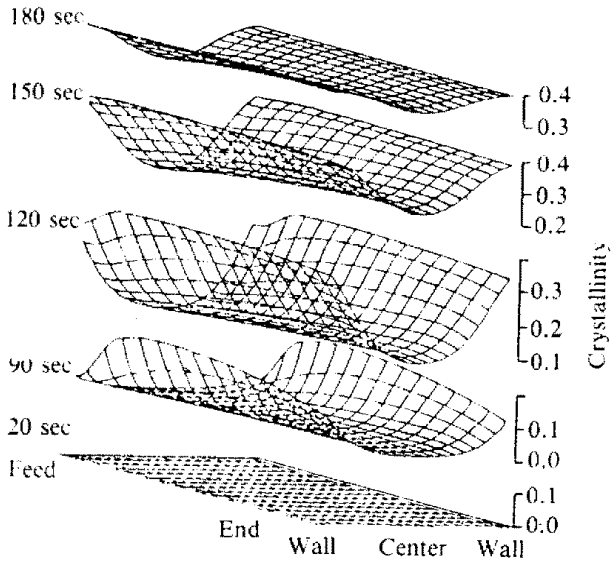

Fig. 8. Change of the crystallinity profile with time.

tion after 100 seconds (Fig. 7) but the equilibrium crystallinity was not obtained even after 180 seconds (Fig. 8).

VITRIFICATION AND PHASE SEPARATION DURING THE RIM PROCESS OF EPOXY RESIN

An engineering analysis of reaction injection molding process of epoxy resin was carried out through numerical simulation and actual experiment (3). In order to simulate the process, the reaction kinetic equation as well as the viscosity function was obtained from the thermal analysis and rheological measurement.

The epoxy resin was composed of the reaction product of the diglycidyl ether of Bisphenol-A (DGEBA; epoxy equivalent of 190) and triethylene tetramine (TETA) with the amount of TETA fixed at 10 phr (parts per hundred parts of DGEBA by weight). The reaction kinetic equation was obtained from the dynamic DSC experiment (4) by measuring the exothermic heat of reaction. As shown in Fig. 9, the vitrification (or solidification) occurred as the

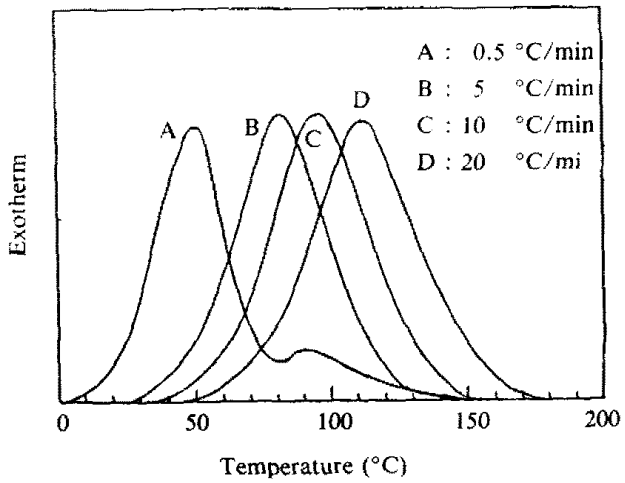

Fig. 9. Thermograrms obtained from the dynamic DSC experiment during the epoxy curing.

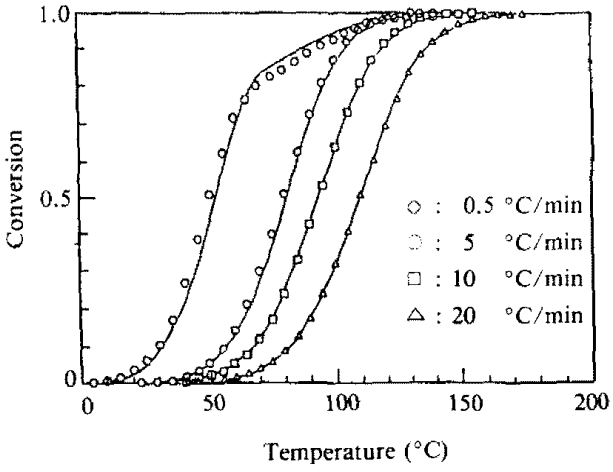

Fig. 11. Experimental conversion data (points) and the conversion calculated from the kinetic equation (lines).

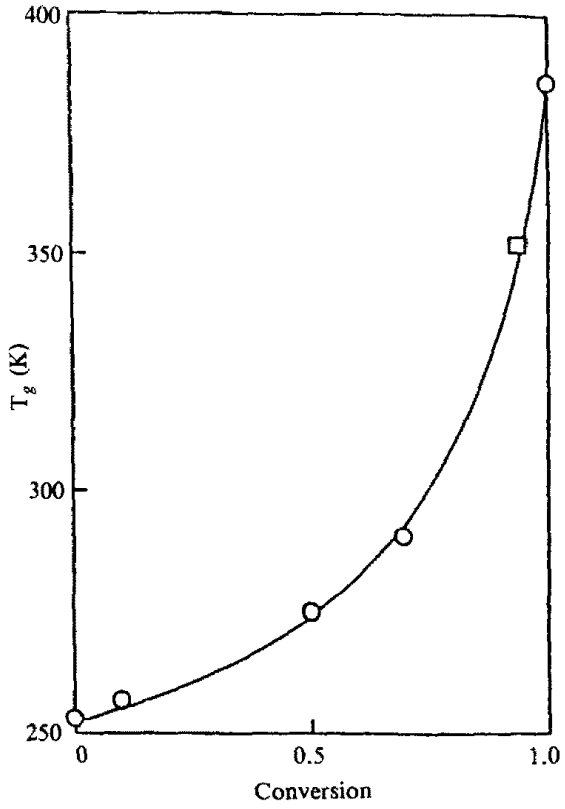

Fig. 10. Glass transition temperature versus conversion from experimental data (solid line represents Di Benedetto's equation).

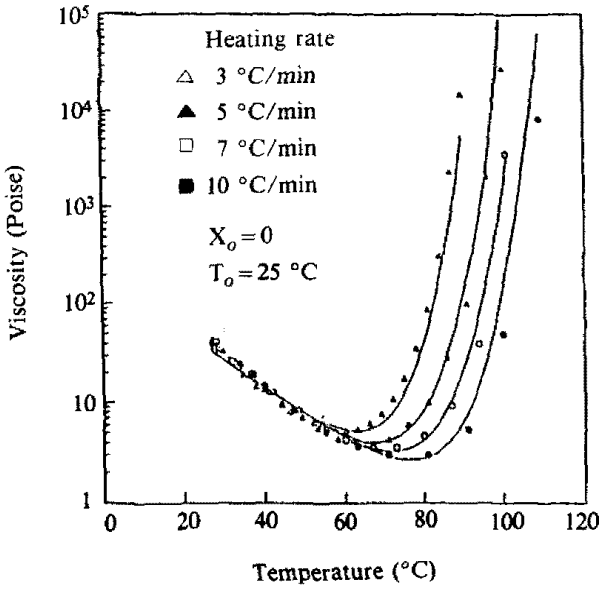

Fig. 12. Viscosity versus temperature plot measure by RMS (points) and calculated from the viscosity function (lines) during the epoxy curing process.

T_g of the reacting mixture exceeded the reaction temperature. When the heating rate was set at 0.5°C/min, the reaction was carried out at low temperature and the reaction rate was slowed due to the vitrification effect at about 50°C. As the sample was heated further the reaction proceeded again as the reaction temperature was increased at above 80°C and the double peak of exotherm was observed.

The glass transition temperature, T_g, of the reacting mixture was measured from the samples obtained by stopping the reaction at different level of conversion (Fig. 10). In orter to describe the T_g change as a function of conversion, Di Benedetto's equation was used to fit the data as Eq. 10.

$$\frac{T_g - T_{go}}{T_{go}} = \frac{(0.3-0.2)\beta}{1-0.8\beta} \tag{10}$$

In order to describe the effect of the vitrification on the reaction rate, the reaction kinetic equation was modified to include the effect of the difference of the T_g of the rection mixture and the reaction temperature. Thus a WLF type frequency factor was added in the equation and the parameters were determined by the regression of the conversion data (Fig. 11) obtained from the DSC exotherm as follows (Eq. 11, 12).

$$\frac{dC^*}{dt} = A_t \exp\left(-\frac{18600}{RT}\right)(1-C^*)^{1.64} \tag{11}$$

$$\ln A_t = \ln(3.83\times 10^8) + \frac{(T-T_g-20)}{2+|T-T_g-20|} \tag{12}$$

The viscosity function was measured with the parallel plate rheometer (Rheometrics Mechanical Spectrometer RMS). The viscosity function was obtained from the reaction kinetic equation and the viscosity measurement by changing the parameters in the viscosity function to fit the rheometer data as shown in Fig. 12 and Eq. 13.

$$\eta = \eta_0 \exp\left(\frac{E_\eta}{RT}\right)\left(5.25C^* - 0.155\left(\frac{C_g^*}{C_g^*-C^*}\right)\right) \tag{13}$$

The computer simulation results (5) on the epoxy RIM process inside a disk type mold utilizing the reaction kinetic equation with the vitrification effect as well as the viscosity function thus obtained, could give informations about the T_g profile within the molded product as a function of time such as shown in Fig. 13.

The addition of the CTBN and ATBN rubber (carboxylated and amine terminated butadiene-acrylonitrile rubber) to enhance the impact resistant properties would make the system more complicated, since the phase separation behavior should also be analyzed. The CTBN and ATBN both show UCST behavior when they were mixed with the epoxy oligomer and the critical temperature increased as the curing reaction proceeded which meant that the compatibility at a given temperature decreased as the molecular weight of the epoxy resin increased (Fig. 14). The phase separation behavior was studied by the laser light scattering method on the polymerizing samples. CTBN rubber (AN%: 17, m.w.: 3,500) and ATBN rubber (AN%: 16, m.w. 3,600) were added in varying amounts and curing reaction was carried out at 70-110°C.

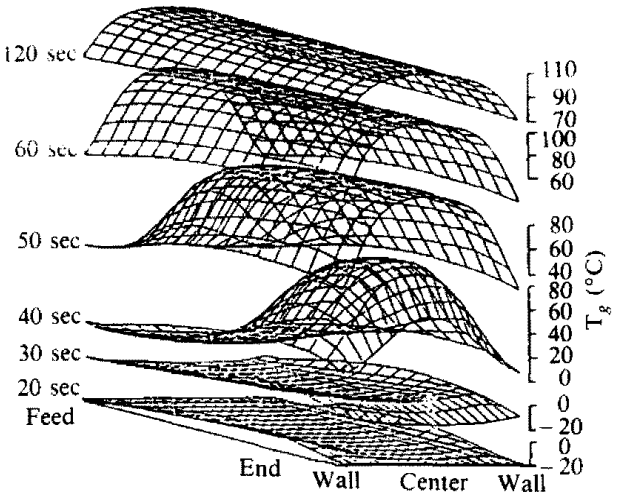

Fig. 13. Change of T_g profile with time during the epoxy RIM process.

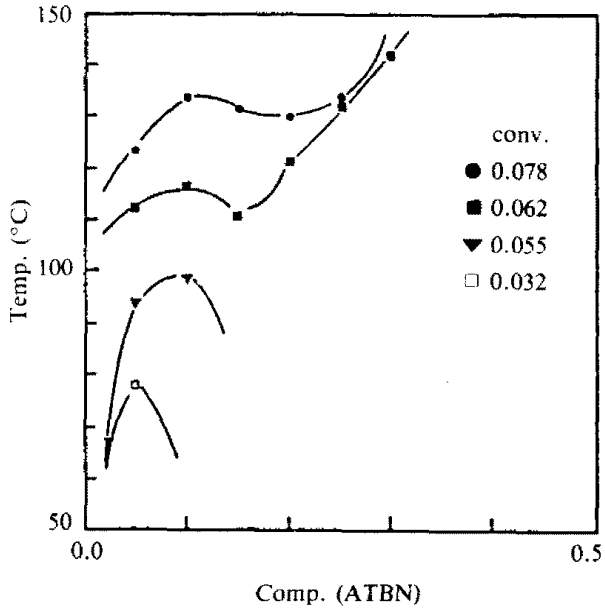

Fig. 14. Cloud point curveswith conversion (mol. wt.) for the DGEBA-ATBN blend.

Fig. 15 shows the typical light scattering result. As the polymerization was proceeded, the scattered light intensity increased and the angle of maximum scattered light also moved towards lower angle. The domain correlation length (md) which was the distance between the center of the neighboring domains (which could be related to the domain size if the concentration of the domain was known), was inversely related to the angle of maximum scattered light intensity, and thus the results showed that the domain size increased up to 3.5 microns at about 5

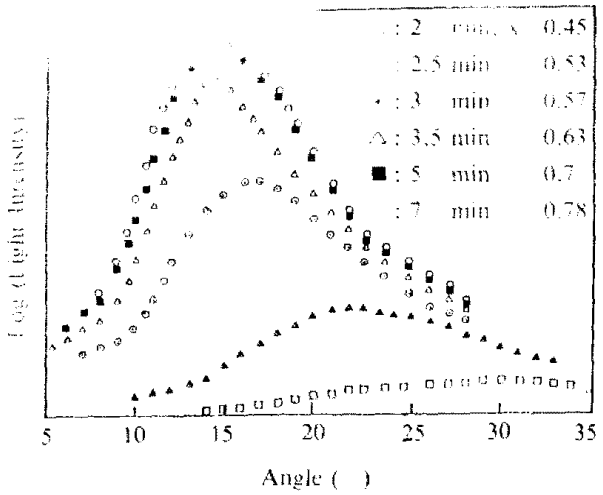

Fig. 15. Scattering light intensity as a function of the scattering angle during the isothermal curing of epoxy resin at 90°C with 15% CTBN.

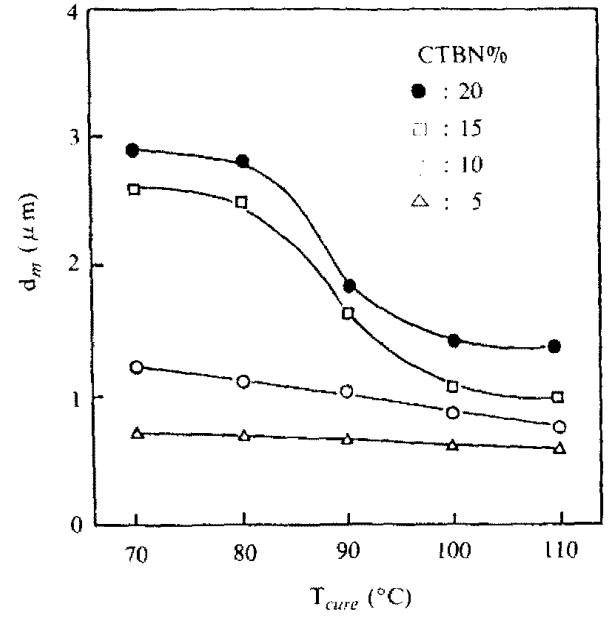

Fig. 16. Change of domain correlation length with the composition and curing temperature.

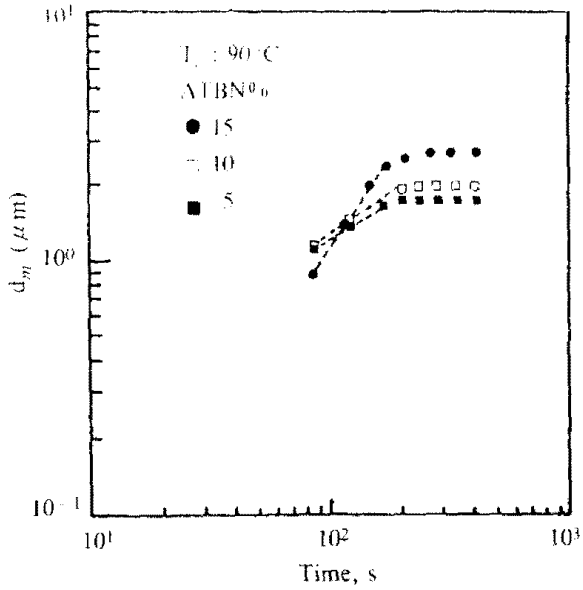

Fig. 17. Change of domain correlation length with different ATBN composition, (T = 90°C).

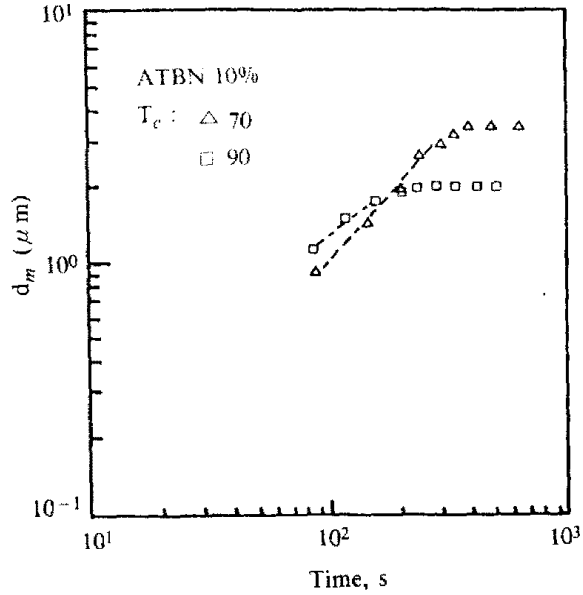

Fig. 18. Change of domain correlation length with different curing temperature (ATBN 10%).

min after the curing had started and remained constant. The domain correlation length could vary at a given CTBN concentration when the curing temperature was changed, in ranges from 1 to 3 microns which could affect the impact strength significantly (Fig. 16).

Fig. 17 shows the growth of the domain corrlation length as a function of the curing time with A TBN content of 5, 10, 15% cured at 90°C. The epoxy blend with higher ATBN concentration showed rapid growth of the rubber domain due to the growing incompatibility of the blend and the final domain size was reached at about 5 min after the curing reaction. The domain growth when cured at different temperature (Fig. 18) shows the effect of the UCST behavior which indicates better compatibility at high temperature. Thus the final domain size reached about 3.5 microns when cured at 70°C but it reached only 2 microns when cured at 90°C although the growth rate of the rubber domain was slower at low

curing temperature because of the high viscosity of the reacting fluid.

NOMENCLATURE

A_i : temperature dependent frequency factor
C^* : extent of reaction $C^* = (C_{ao} - C_a)/C_{ao}$
C_a : concentration of reactant A, g/cm³
C_g^* : extent of reaction at gel point
E_d : activation energy of diffusion for crystallization, cal/mol
R : gas constant, 1.987 cal/gmol °K
T_g : glass transition temperature
T_{go} : glass transition temperature at zero conversion
T_k : temperature of miximum crystal growth rate
T_m : melting point
α : degree of crystallinity
α_{eq} : equilibrium crystallinity
β : conversion
β_{ci} : conversion at which crystallization was started
: constant of supercooling effect

REFERENCES

1. Lee K.H. and Kim S.C., *Polym. Eng. Sci.*, **28**(1), 3 (1988).
2. Lee K.H. and Kim S.C., *Polym. Eng. Sci.*, **28**(7), 477 (1988).
3. Kim D.H. and Kim S.C., *Polymer Composites*, **8**(3), 208 (1987).
4. Kim D.H. and Kim S.C., *Polymer Bulletin*, **18**, 533 (1987).
5. Kim D.H. and Kim S.C., *Polym. Eng. Sci.*, **29**(7), 456 (1989).
6. Kim D.H., "A Study on the Reaction Injection Molding Process and the Phase Separation Behavior of Epoxy Resin", PhD Thesis, KAIST, 1988.
7. Kim D.S., "Curing and Phase Separation Behavior of Epoxy Resin Modified with ATBN", MS Thesis, KAIST, 1989.